Stacking Interactions

DOI: 10.1002/ange.201109074

Oligothiophene Cruciform with a Germanium Spiro Center: A Promising Material for Organic Photovoltaics**

Iain A. Wright, Alexander L. Kanibolotsky, Joseph Cameron, Tell Tuttle, Peter J. Skabara, Simon J. Coles, Calvyn T. Howells, Stuart A. J. Thomson, Salvatore Gambino, and Ifor D. W. Samuel**

Dedicated to Professor Klaus Müllen on the occasion of his 65th birthday

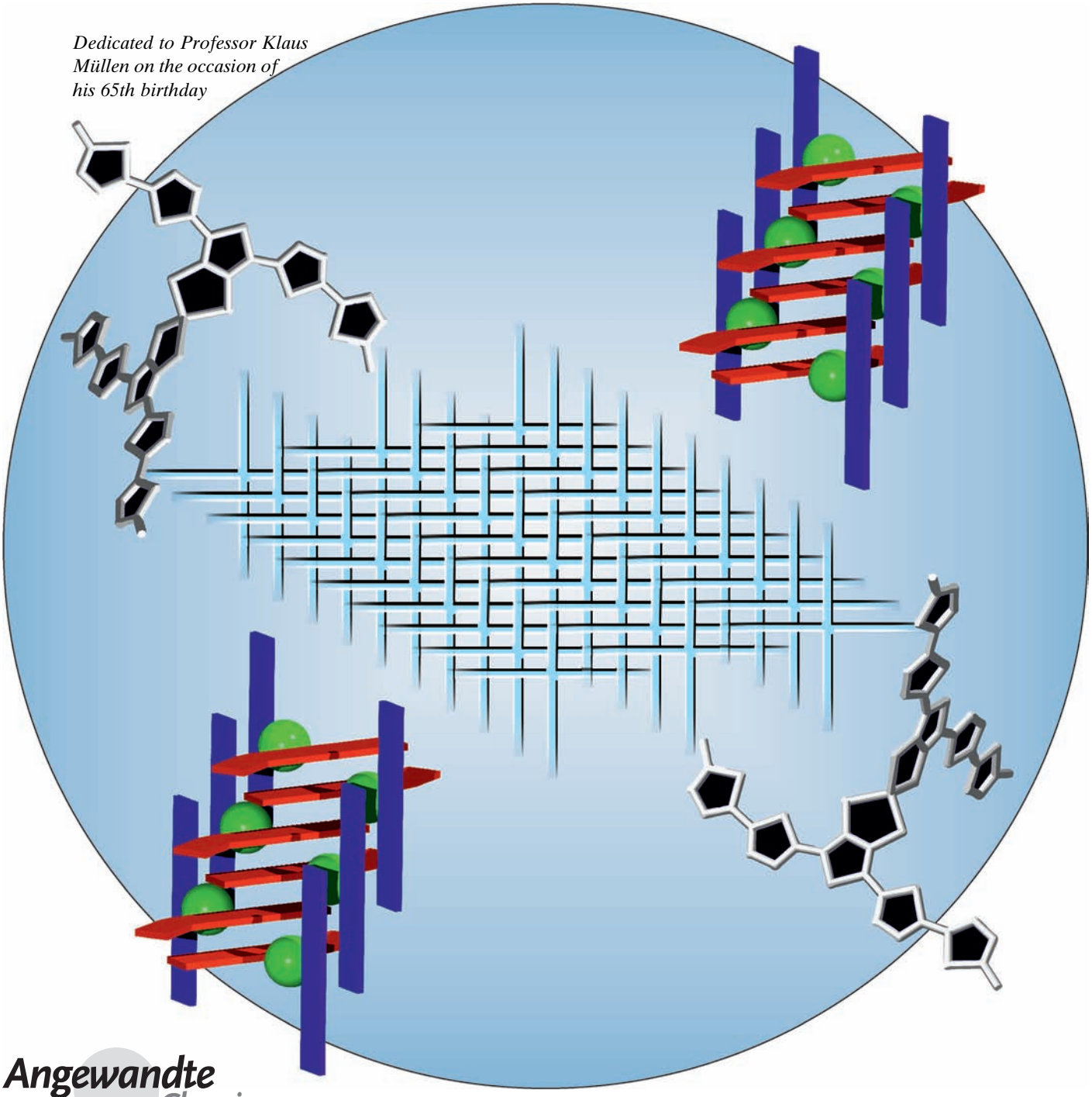

Solution-processable bulk heterojunction (BHJ) solar cells offer a promising technology for solar energy conversion because of their low-cost fabrication, light weight, and potential use in large-area flexible devices. Most of the research in the field of organic photovoltaics (OPVs) has been focused on developing solar cells with a conjugated polymer (CP) as a donor compound. The ability of a polymer/fullerene acceptor blend to form a bicontinuous interpenetrating nanoscale network which provides efficient exciton dissociation and charge transport[1] has made polymeric donors the most promising materials for photovoltaic devices. At present the best solar cells with this type of donor exhibit power conversion efficiencies (PCE) of 8–9 %,[2] which is close to the desired 10 % PCE milestone.[3]

In spite of their superior film-forming properties, polymeric materials suffer from molecular weight polydispersity, end group variation, and batch reproducibility. Small-molecule donors and oligomers with well-defined structures, on the other hand, offer the advantage of creating materials from monodisperse compounds with completely reproducible properties. Small molecules are more prone to self-assemble into ordered domains, thus yielding high charge-carrier mobility of the material and improved performance of OPV devices.[4] At present the best solution-processable BHJ solar cells having small-molecule donors demonstrate PCEs of 4–6.7 % for molecules having a narrow HOMO–LUMO gap.[5] One major advantage of small molecules over polymers is their superior levels of crystallinity, and there is great interest in new strategies for directed self-assembly. Oligothiophenes have been actively investigated as conjugated materials for electronic devices[6] but they usually exhibit wider band gaps than polymers and show lower performance in OPV devices. The processing of oligothiophenes has generally favored evaporation techniques for unsubstituted derivatives as a means of obtaining higher order in the deposited films. For example, whilst it is possible to exceed 2 % efficiency in solar cells fabricated by the vacuum deposition of sexithiophene and C_{70},[7] a solution-processed cell with a blend of α,ω-dihexylsexithiophene/$PC_{61}BM$ ([6,6]-phenyl C_{61}-butyric acid methyl ester) has a PCE of only 0.01 %.[8]

One method for improving OPV performance is to increase the dimensionality of the donor molecules through self-assembly to match it with the intrinsically three-dimensional (3D) character of intermolecular interactions in the fullerene acceptor phase. The increased dimensionality of star-shaped systems has been the subject of intense research in the last decade.[9] The effect of extending the dimensionality of the donor molecule upon OPV performance was first exploited by Roncali and co-workers.[10] By switching to a tetrahedral star-shaped silicon-centered system (**SI1**; see Chart S1 in the Supporting Information), with an absorption cut-off of $\lambda = 440$ nm, they achieved a PCE of 0.3 %.[11] Recently, a similar 3D system (**SI2**) has been used in solution-processed solar cells with $PC_{71}BM$ and demonstrated a PCE of 1.4 %.[12] With the same acceptor, a X-shaped oligothiophene (**SI3**) has shown a PCE of 1.54 %.[13] The most pronounced effect of extending dimensionality upon OPV performance was achieved by using a dendrimeric oligothiophene (**SI4**) and $PC_{61}BM$ which yielded an efficiency of 1.7 %.[14]

Although the 3D architectures of the aforementioned oligothiophenes provide motifs for the most isotropic charge-transporting properties, the most efficient aggregation can be achieved from two-dimensional (2D) π–π stacking in mutually orthogonal directions. An example of such a stacking interaction was demonstrated earlier in the crystal structure of 2,6-bis-(4-hexylthiophen-2-yl)-benzo[1,2-d;4,5-d′]bisthiazole (**1**; Scheme 1), wherein assembly in the third dimension and the origin of an orthogonal arrangement has been provided by noncovalent sulfur–nitrogen interactions[15] (Figure 1 a). Fixing such a cruciform arrangement of two mutually orthogonal conjugated backbones by covalent bonding would create a much more stable tecton for such supramolecular assembly and provide the possibility for electronic conjugation between the arms within the molecule. Spiro-centered X-shaped systems or other types of cruciforms[16] seem to be ideal structures for this. Cruciform conjugated oligomers having a C or Si spiro center are usually considered to be two independent oligomers with no electronic communication, although some conjugation is possible [e.g., in 9,9′-spirobifluorene and 9,9′-spirobi(9-silafluorene)]; if the terminal p_π-atomic orbitals around the spiro center in each of the two orthogonal conjugated systems are antisymmetric to one another,[17] the value of the coupling is higher for the more compact carbon spiro center.[18]

Recently, we reported the synthesis of a monodisperse hybrid compound bearing two septithiophene fragments bridged with a fused tetrathiafulvalene (TTF) unit (**2**; Scheme 1), which exhibits complex redox behavior and can be oxidized up to the octacation.[19] The end-capped oligothiophene **3** having a fused dithiolone unit is similar to that of **4**, which was used for the synthesis of compound **2**. Both compounds can be used as synthetic equivalents of dinucleophilic synthons for constructing a series of spiro structures with the sulfur handles providing space separation of the two conjugated backbones and the possibility for spiro conjugation.

[*] Dr. I. A. Wright, Dr. A. L. Kanibolotsky, J. Cameron, Dr. T. Tuttle, Prof. Dr. P. J. Skabara
WestCHEM, Department of Pure and Applied Chemistry
University of Strathclyde, Glasgow G1 1XL (UK)
E-mail: peter.skabara@strath.ac.uk
Dr. A. L. Kanibolotsky
Institute of Physical-Organic Chemistry and Coal Chemistry
83114 Donetsk (Ukraine)
Dr. S. J. Coles
School of Chemistry, University of Southampton
Highfield, Southampton, SO17 1BJ (UK)
C. T. Howells, S. A. J. Thomson, Dr. S. Gambino, Prof. Dr. I. D. W. Samuel
Organic Semiconductor Centre, SUPA, School of Physics & Astronomy, University of St Andrews
St Andrews, KY16 9SS (UK)
E-mail: idws@st-and.ac.uk

[**] The authors thank the EPSRC for funding.
Supporting information for this article is available on the WWW under http://dx.doi.org/10.1002/anie.201109074.

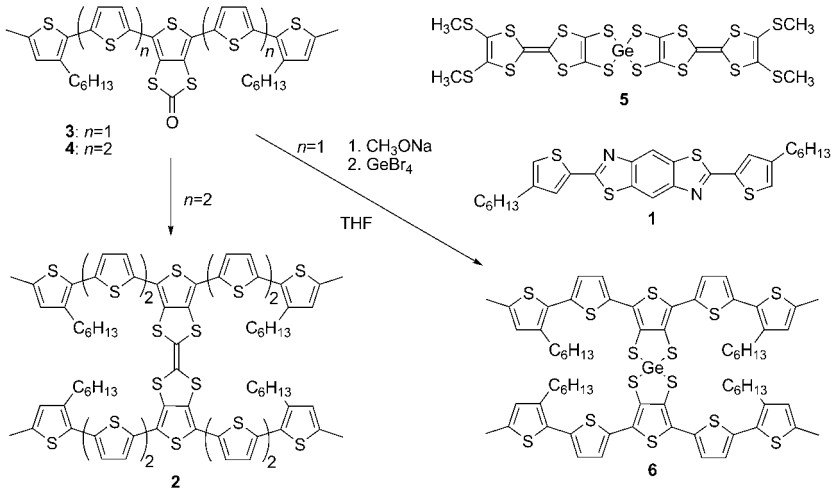

Scheme 1. Oligothiophenes **3** and **4** as starting compounds for constructing **2** and Ge cruciform **6**, and previously reported electroactive compounds **1** and **5**.

synthetic procedures and characterization for all new compounds are given in the Supporting Information. Compounds **3** and **6** have been studied by cyclic voltammetry and absorption spectroscopy. The hole mobility has been determined for these compounds by charge-generation layer time-of-flight (TOF) measurements. The structure of **6** was investigated by single-crystal X-ray analysis (CCDC 853611), and photovoltaic devices were fabricated using blends of compound **6** with $PC_{71}BM$.

Cyclic voltammetry revealed one reversible and one quasireversible oxidation wave for the oligothiophene **3** (Table 1), and corresponds to the formation of a cation radical and dication, respectively. Upon oxidation, compound **6** showed three quasireversible waves and one irreversible

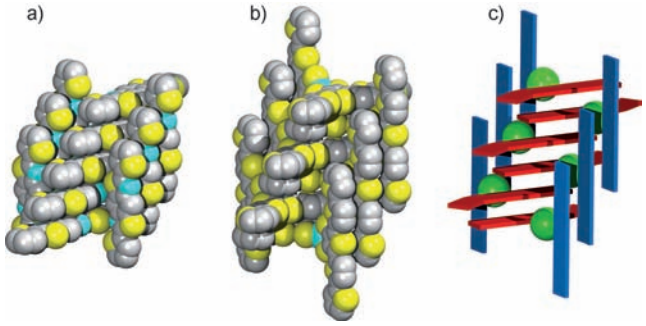

Figure 1. Space-filling model of 2D π–π stacking for compounds **1** (a) and **6** (b). The alkyl substituents and hydrogen atoms are omitted for clarity. c) Schematic representation of intermolecular interactions for compound **6**. Green: GeS_4 spiro center, red: oligothiophenes which stack in a vertical direction with an interplanar distance of 3.417 Å, blue: quinquithiophenes with a stacking distance of 3.704 Å in the horizontal direction.

Table 1: UV absorbance and electrochemical properties of compounds **3** and **6**.

	λ_{max} [nm]	HOMO–LUMO[a] [eV]	HOMO[b] [eV]	LUMO[b] [eV]	E_{ox} [V][c]	E_{red} [V]
3	435	2.44 (2.33)	−5.21	−2.88	0.52/0.47 0.66/0.59	−2.03
6	430	2.47 (1.36)	−5.00	−3.64	0.29/0.25 0.44/0.34 0.70/0.64 1.14	−1.49

[a] HOMO–LUMO gap was calculated from the absorption onset; the electrochemical gap is shown within parentheses and was calculated as the difference between the HOMO and LUMO levels given in the next two columns. [b] HOMO (LUMO) level was found from the onset of oxidation (reduction) and referenced to Fc/Fc^+. [c] In the case of reversible (quasireversible) oxidation the position of the peak in the anodic/cathodic cycle is given.

For efficient charge transport, the conjugation between the two orthogonal backbones in a spiro system is of great importance. In contrast, for efficient intermolecular interactions the two conjugated parts of the cruciform should be separated from each other by a sufficient distance. Taking this into account, Ge has certain advantages over C or Si as spiro centers. It gives better spatial separation of oligomers in the spiro structure and has a full d-shell which might participate in spiro conjugation. Since the first synthesis of bis(dithiolate) compounds with Si, Ge, Sn, and Pb spiro centers in 1966,[20] only a few examples of bis(dithiolate)germanium(IV) have been reported,[21] including the fused spirobi-[(1,3,2)dithiagermole] TTF system **5**.[22] To the best of our knowledge, no such materials have been studied in organic electronic applications.

With the above in mind we synthesized the fused spirobi-[(1,3,2)dithiagermole]quinquithiophene system **6** by treating dithiolone **3** with sodium methoxide and reacting the resulting sodium dithiolate with germanium (IV) bromide. The full

wave (Table 1, and Figure SI4a in the Supporting Information), which could be attributed to sequential transitions to the cation radical ($\mathbf{6}^{+\bullet}$), bis(cation radical) ($\mathbf{6}^{+\bullet,+\bullet}$), cation radical/dication ($\mathbf{6}^{+\bullet,2+}$), and bis(dication) ($\mathbf{6}^{2+,2+}$). Compounds **3** and **6** both gave one irreversible reduction wave.

The large decrease in the energy level of the LUMO in going from oligothiophene **3** to **6**, together with a destabilization of the HOMO, results in a greater than 1 eV discrepancy between optically and electrochemically determined HOMO–LUMO gaps for the cruciform **6**. The optically measured HOMO–LUMO gap represents exclusively the π→π* transition of the quinquithiophene chain, so the observed electrochemistry suggests that the Ge spiro center is an electroactive subunit within the parent compound: whilst the difference in HOMOs between both compounds could be due to substituent effects (carbonyl versus Ge), the large variance in the LUMOs points towards the Ge center as a contributing redox site for reduction.

Previously it has been suggested that conjugated cruciform oligomers are not prone to aggregation.[17,23] In contrast,

the Ge cruciform exhibited distinct signs of aggregation similar to those observed earlier for hybrid TTF/oligothiophene compounds.[19,24] To disrupt aggregation in solution (e.g., for solution state NMR experiments and solution processing), it was necessary to add a small amount of CS_2.

Crystals of compound **6** suitable for X-ray analysis were grown by slow liquid diffusion of ethanol into a CH_2Cl_2/CS_2 (3:1) solution. Figures 1a and b show the 2D stacking in the crystals of compounds **1** and **6**, respectively. For the latter, the crystal structure revealed two types of stacking interactions. The oligothiophene of each cruciform molecule containing a bithiophene unit in a *syn*-orientation within the central part of the chain (see red plates with a small twist on one end; Figure 1c) is involved in a stacking interaction with an identical chain of another molecule. These two molecules relate to each other by a center of symmetry, which means that the other part of the cruciform (quinquithiophene represented by blue vertical plates in Figure 1c) is located on different sides from the site of the π–π stacking. These quinquithiophenes stack in a second, perpendicular orientation with translation space symmetry. The interplane distances for these two types of stacking are 3.417 Å and 3.704 Å, respectively.

We applied computational methods to probe the effect of the Ge cruciform center on the electronic properties of the whole molecule. All structures were optimized using the B97-D[25] functional as implemented in TURBOMOLE 6.3.1.[26] Monomers were optimized using both def2-TZVP[27] and def2-SVP basis sets,[27] whilst dimers and tetramers were optimized using the def2-SVP basis set. These calculations were carried out using the RI-J approximation,[28] whilst optimizations on tetramer structures were also carried out using MARI-J approximation.[29] NBO analyses were carried out in Gaussian 09[30] by performing single-point energy calculations on optimized structures using the M06L functional[31] with the 6-31(d) basis set.[32]

The hexyl chain from the experimental system was shortened to a methyl group in the computational model to decrease the computational costs associated with the model. The structure of the optimized monomer showed twists in the quinquithiophene arms, whilst the structure obtained from crystallographic data showed the arms of the cruciform to be more planar. The twisting of the quinquithiophene arms in the monomer structure is due to the ability of the arms to form stabilizing intramolecular interactions with each other. However, these intramolecular interactions are relatively weak when compared to the much stronger intermolecular π–π stacking interactions that are available if the arms are properly aligned when the monomers dimerize. Therefore, the intramolecular destabilization (straightening of the quinquithiophene arms) that occurs when the monomers dimerize is easily compensated for by the much stronger intermolecular interactions formed in the complex. One aspect to note from the monomer study is the partial occupancy of the LUMO over the GeS_4 central unit (see Figure SI6 and Table SI1 in the Supporting Information), which supports the surprisingly low reduction potential of **6** relative to that of **3**. In addition, as a result of the symmetry of the orbitals the degenerate LUMO + 1 orbital also shows delocalization over the GeS_4 unit (see Figure SI6 in the Supporting Information; also shown are the degenerate HOMO and HOMO−1 orbitals). In this comparison it is important to remember that the solution state CV of the substrate is representative of the computational focus on the monomer unit as a non-aggregating species.

The optimized dimer structure of the Ge cruciform indicates that the vertical arms have a slight bend towards the stacked arms to gain more favorable stacking interactions (see Figure SI6 in the Supporting Information). While the degeneracy of the LUMO and LUMO + 1 orbitals are retained in the Ge cruciform dimer, the dimerization of the cruciforms has the effect of perturbing the degeneracy of the HOMO and HOMO−1 (Figure SI7). However, in a large network of stacked cruciform species, it is unlikely that this would occur as the vertical arms are also involved in stacking with adjacent molecules. Nonetheless, the optimized dimers provide a reasonable representation of the stacking interaction that stabilizes the formation of the extended cruciform structure. The binding energy (ΔE_b) for the dimer was calculated at the B97-D/def2-SVP level of theory and was found to be $\Delta E_b = 52.1\ \text{kcal mol}^{-1}$.

The binding energy represents the relative energy of the dimer to the free monomers. However, as discussed in the case of the monomers, the conformation of the free monomer differs significantly from that observed in the extended structure. Therefore, to determine the interaction energy (ΔE_{int}) between the monomer units within the network, single-point energy calculations were performed on the monomer units using their geometry obtained from the dimer optimizations. The interaction energy calculated in this way is increased relative to the binding energy because of the decreased stability of the monomer units extracted from the optimized dimers. The interaction energy of the Ge cruciform is $\Delta E_{int} = 63.0\ \text{kcal mol}^{-1}$.

The optimized tetramer structure of the Ge cruciform (Figure 2) is similar to the structure determined by crystallography. The bending of the quinquithiophene arms present in the optimized dimer structures is not present in the tetramer structures because of the fact that there are stacking interactions in two dimensions. There is very little difference in binding energy ($\Delta E = 200.9\ \text{kcal mol}^{-1}$) and interaction energy ($\Delta E = 207.2\ \text{kcal mol}^{-1}$) within the Ge cruciform

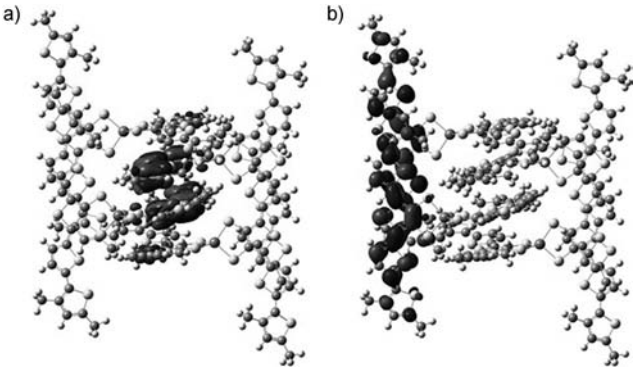

Figure 2. a) HOMO of Ge cruciform tetramer. b) LUMO of Ge cruciform tetramer.

tetramer, which indicates an increased stability of the monomer unit in the tetramer arrangement, relative to the dimer.

The HOMOs of the tetramers (Figure 2a) show that electron density is concentrated in the middle of the tetramer, between two horizontally stacked quinquithiophene chains. As in the case of the dimer, the aggregation of the cruciform units results in a loss of degeneracy between the HOMO and HOMO−1 orbitals, whereas the LUMO and LUMO+1 orbitals remain degenerate (see Figure SI8 in the Supporting Information). The LUMOs of the tetramers (Figure 2b), are also very similar to each other, both situated on the vertically stacked arms. This result again demonstrates that there is some degree of charge transfer upon excitation, which may yield good excimer diffusion through the material in two dimensions.

In parallel, a computational study was carried out to compare the properties of the Ge cruciform and an analogous Si-centered structure to determine the effect of varying the central atom with other group 14 elements. We found that the closely related Si structure would also be worth synthesizing and studying and our reasoning is explained in the Supporting Information.

The effect of the stacking pattern on the mobility of holes was measured by the charge-generation layer TOF technique. TOF measurements measure charge mobility in the direction perpendicular to the film, which is the direction most relevant to solar cells. It was found that both the Ge cruciform **6** and its precursor **3** show dispersive charge transport. The transient photocurrent measured for **3** and **6** at an applied electric field of $1.1\times10^5\ \mathrm{V\,cm^{-1}}$ is shown on a log-log scale in Figure 3. The

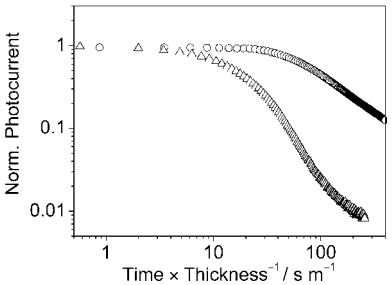

Figure 3. Normalized hole photocurrent transients for compounds **3** (circles) and **6** (triangles) measured at an electric field of $1.1\times10^5\ \mathrm{V\,cm^{-1}}$ and plotted on a log-log scale. The thickness of the film of **3** was 230 nm, and that of **6** was 350 nm.

transit time (of charges across the film) is determined from the knee in the double log plots and found to be 9.3 μs for the precursor **3**, and 7 μs for **6**. This leads to mobility values of $2.2\times10^{-5}\ \mathrm{cm^2\,V^{-1}\,s^{-1}}$ for the precursor **3** and $4.2\times10^{-5}\ \mathrm{cm^2\,V^{-1}\,s^{-1}}$ for **6**. For compound **1** the transit time was 11 μs, thus giving a mobility of $6\times10^{-6}\ \mathrm{cm^2\,V^{-1}\,s^{-1}}$ (data not shown).

These results show that the 2D stacking of **6** is beneficial for charge transport. It is interesting to compare these results with other mobility measurements in the direction perpendicular to the film on related materials. Highly dispersive charge transport has already been observed in the case of **2** and septithiophene **4**,[19] thus leading to a mobility value of $1.2\times10^{-6}\ \mathrm{cm^2\,V^{-1}\,s^{-1}}$ for **4** and $2.5\times10^{-6}\ \mathrm{cm^2\,V^{-1}\,s^{-1}}$ for **2**.[19] The mobility of **6** is an order of magnitude higher than that reported for sexithiophene,[33] and the same order of magnitude as that reported for poly(3-hexylthiophene).[34]

To demonstrate that the stacking structure is suitable for organic electronic devices, we made BHJ solar cells containing the Ge cruciform **6** as the donor and $PC_{71}BM$ as the acceptor. The device characteristics at different blend ratios are presented in Chart S2 of the Supporting Information. Compound **6** exhibited a maximum PCE of 2.26% for a 1:6 blend ratio. This result is very encouraging considering that **6** has a wide band gap, with an absorption onset of $\lambda = 502$ nm. It compares favorably with reports on sexithiophene solar cells. Muhammad et al. recently reported a power conversion efficiency of 0.01% for a solution-processed sexithiophene-based solar cell.[8] Sakai et al. obtained 2.38% efficiency in a sexithiophene solar cell, but their device required fabrication by evaporation.[7] Hence our results show that the cruciform not only gives improved mobility but also improved performance of solution-processed solar cells. By reducing the energy gap, whilst retaining the cruciform structure, considerable improvements in efficiency can be expected.

Received: December 22, 2011
Published online: March 30, 2012

Keywords: aggregation · germanium · oligomerization · spiro compounds · stacking interactions

[1] B. Kippelen, J.-L. Bredas, *Energy Environ. Sci.* **2009**, *2*, 251 – 261.
[2] N. Jenny, *Mater. Today* **2011**, *14*, 462 – 470.
[3] C. J. Brabec, S. Gowrisanker, J. J. M. Halls, D. Laird, S. Jia, S. P. Williams, *Adv. Mater.* **2010**, *22*, 3839 – 3856.
[4] a) M. T. Lloyd, J. E. Anthony, G. G. Malliaras, *Mater. Today* **2007**, *10*, 34 – 41; b) A. Mishra, P. Bäuerle, *Angew. Chem.* **2012**, *124*, 2060 – 2109; *Angew. Chem. Int. Ed.* **2012**, *51*, 2020 – 2067.
[5] a) B. Walker, C. Kim, T.-Q. Nguyen, *Chem. Mater.* **2011**, *23*, 470 – 482; b) B. Walker, A. B. Tomayo, X.-D. Dang, P. Zalar, J. H. Seo, A. Garcia, M. Tantiwiwat, T.-Q. Nguyen, *Adv. Funct. Mater.* **2009**, *19*, 3063 – 3069; c) Y. Matsuo, Y. Sato, T. Niinomi, I. Soga, H. Tanaka, E. Nakamura, *J. Am. Chem. Soc.* **2009**, *131*, 16048 – 16050; d) H. Shang, H. Fan, Y. Liu, W. Hu, Y. Li, X. Zhan, *Adv. Mater.* **2011**, *23*, 1554 – 1557; e) Y. Sun, G. C. Welch, W. L. Leong, C. J. Takacs, G. C. Bazan, A. J. Heeger, *Nat. Mater.* **2012**, *11*, 44 – 48.
[6] A. Mishra, C.-Q. Ma, P. Bauerle, *Chem. Rev.* **2009**, *109*, 1141 – 1276.
[7] J. Sakai, T. Taima, T. Yamanari, K. Saito, *Sol. Energy Mater.* **2009**, *93*, 1149 – 1153.
[8] F. F. Muhammad, K. Sulaiman, *Thin Solid Films* **2011**, *519*, 5230 – 5233.
[9] a) A. L. Kanibolotsky, I. F. Perepichka, P. J. Skabara, *Chem. Soc. Rev.* **2010**, *39*, 2695 – 2728; b) J. Roncali, P. Leriche, A. Cravino, *Adv. Mater.* **2007**, *19*, 2045 – 2060.
[10] S. Roquet, R. de Bettignies, P. Leriche, A. Cravino, J. Roncali, *J. Mater. Chem.* **2006**, *16*, 3040 – 3045.
[11] J. Roncali, P. Frere, P. Blanchard, R. de Bettignies, M. Turbiez, S. Roquet, P. Leriche, Y. Nicolas, *Thin Solid Films* **2006**, *511*, 567 – 575.

[12] E. A. Kleymyuk, P. A. Troshin, E. A. Khakina, Y. N. Luponosov, Y. L. Moskvin, S. M. Peregudova, S. D. Babenko, T. Meyer-Friedrichsen, S. A. Ponomarenko, *Energy Environ. Sci.* **2010**, *3*, 1941 – 1948.
[13] H. Shang, H. Fan, Y. Liu, W. Hu, Y. Li, X. Zhan, *J. Mater. Chem.* **2011**, *21*, 9667 – 9673.
[14] C.-Q. Ma, M. Fonrodona, M. C. Schikora, M. M. Wienk, R. A. J. Janssen, P. Bauerle, *Adv. Funct. Mater.* **2008**, *18*, 3323 – 3331.
[15] H. Pang, F. Vilela, P. J. Skabara, J. J. W. McDouall, D. J. Crouch, T. D. Anthopoulos, D. D. C. Bradley, D. M. De Leeuw, P. N. Horton, M. B. Hursthouse, *Adv. Mater.* **2007**, *19*, 4438 – 4442.
[16] A. Zen, A. Bilge, F. Galbrecht, R. Alle, K. Meerholz, J. Grenzer, D. Neher, U. Scherf, T. Farrell, *J. Am. Chem. Soc.* **2006**, *128*, 3914 – 3915.
[17] T. P. I. Saragi, T. Spehr, A. Siebert, T. Fuhrmann-Lieker, J. Salbeck, *Chem. Rev.* **2007**, *107*, 1011 – 1065.
[18] A. Schweig, U. Weidner, D. Hellwinkel, W. Krapp, *Angew. Chem.* **1973**, *85*, 360 – 361; *Angew. Chem. Int. Ed. Engl.* **1973**, *12*, 310 – 311.
[19] I. A. Wright, P. J. Skabara, J. C. Forgie, A. L. Kanibolotsky, B. Gonzalez, S. J. Coles, S. Gambino, I. D. W. Samuel, *J. Mater. Chem.* **2011**, *21*, 1462 – 1469.
[20] a) F. H. Fink, J. A. Turner, D. A. Payne, *J. Am. Chem. Soc.* **1966**, *88*, 1571 – 1572; b) D. A. Payne, F. H. Fink, *J. Chem. Educ.* **1966**, *43*, 654.
[21] a) H. Lavayssière, G. Dousse, J. Satge, *Recl. Trav. Chim. Pays-Bas* **1988**, *107*, 440 – 448; b) J. Pfeiffer, M. Noltemeyer, A. Meller, *Z. Anorg. Allg. Chem.* **1989**, *572*, 145 – 150.
[22] K. Ueda, M. Yamanoha, T. Sugimoto, H. Fujita, A. Ugawa, K. Yakushi, K. Kano, *Chem. Lett.* **1997**, 461 – 462.
[23] J. Pina, J. Seixas de Melo, H. D. Burrows, A. Bilge, T. Farrell, M. Forster, U. Scherf, *J. Phys. Chem. B* **2006**, *110*, 15100 – 15106.
[24] A. L. Kanibolotsky, L. Kanibolotskaya, S. Gordeyev, P. J. Skabara, I. McCulloch, R. Berridge, J. E. Lohr, F. Marchioni, F. Wudl, *Org. Lett.* **2007**, *9*, 1601 – 1604.
[25] S. Grimme, *J. Comput. Chem.* **2006**, *27*, 1787 – 1799.
[26] R. Ahlrichs, M. Bar, M. Haser, H. Horn, C. Kolmel, *Chem. Phys. Lett.* **1989**, *162*, 165 – 169.
[27] F. Weigend, R. Ahlrichs, *Phys. Chem. Chem. Phys.* **2005**, *7*, 3297 – 3305.
[28] M. Feyereisen, G. Fitzgerald, A. Komornicki, *Chem. Phys. Lett.* **1993**, *208*, 359 – 363.
[29] M. Sierka, A. Hogekamp, R. Ahlrichs, *J. Chem. Phys.* **2003**, *118*, 9136 – 9148.
[30] Gaussian.
[31] Y. Zhao, D. G. Truhlar, *J. Chem. Phys.* **2006**, *125*, 194101 – 194111.
[32] M. J. Frisch, J. A. Pople, J. S. Binkley, *J. Chem. Phys.* **1984**, *80*, 3265 – 3269.
[33] P. Delannoy, G. Horowitz, H. Bouchriha, F. Deloffre, J. L. Fave, F. Garnier, R. Hajlaoui, M. Heyman, F. Kouki, J. L. Monge, P. Valat, V. Wintgens, A. Yassar, *Synth. Met.* **1994**, *67*, 197 – 200.
[34] a) A. J. Mozer, N. S. Sariciftci, A. Pivrikas, R. Osterbacka, G. Juska, L. Brassat, H. Bassler, *Phys. Rev. B* **2005**, *71*, 035214; b) N. T. Binh, L. Q. Minh, H. Bassler, *Synth. Met.* **1993**, *58*, 39 – 50.

